

Inelastic Electron-Proton and γ -Proton Scattering and the Structure of the Nucleon*

J. D. BJORKEN AND E. A. PASCHOS

Stanford Linear Accelerator Center, Stanford University, Stanford, California 94305

(Received 10 April 1969)

A model for highly inelastic electron-nucleon scattering at high energies is studied and compared with existing data. This model envisages the proton to be composed of pointlike constituents ("partons") from which the electron scatters incoherently. We propose that the model be tested by observing γ rays scattered inelastically in a similar way from the nucleon. The magnitude of this inelastic Compton-scattering cross section can be predicted from existing electron-scattering data, indicating that the experiment is feasible, but difficult, at presently available energies.

I. INTRODUCTION

ONE of the most interesting results emerging from the study of inelastic lepton-hadron scattering at high energies and large momentum transfers is the possibility of obtaining detailed information about the structure, and about any fundamental constituents, of hadrons. We discuss here an intuitive but powerful model, in which the nucleon is built of fundamental pointlike constituents. The important feature of this model, as developed by Feynman, is its emphasis on the infinite-momentum frame of reference.

It is argued that when the inelastic scattering process is viewed from this frame, the proper motion of the constituents of the proton is slowed down by the relativistic time dilatation, and the proton charge distribution is Lorentz-contracted as well. Then, under appropriate experimental conditions, the incident lepton scatters instantaneously and incoherently from the individual constituents of the proton, assuming such a concept makes sense.

We were greatly motivated in this investigation by Feynman, who put the above ideas into a highly workable form. In Sec. II, we discuss the basic ideas and equations for the model as they apply to electron-proton scattering. Two models are then discussed in detail, with interesting consequences for the ratio of electron-proton and electron-neutron scattering. For a broad class of such models, we find a sum rule which indicates that, although it is not difficult to fit the data within $\sim 50\%$, it is more difficult to do better; the observed cross section is uncomfortably small.

In Sec. III, we look for stringent tests of Feynman's picture. We propose that, under similar experimental conditions, inelastic Compton scattering can also be calculated within the model. It is shown that the ratio of inelastic electron-proton to inelastic γ -proton scattering, under identical kinematical conditions, is model-independent and of order unity, provided the proton constituents (which Feynman calls "partons") possess unit charge and spin 0 or $\frac{1}{2}$. We propose experiments which can measure inelastic Compton scattering. To this end we have estimated the yield and background

curves, and we conclude that such experiments may be feasible at energies available to SLAC.

II. INELASTIC e - p SCATTERING

The basic idea in the model is to represent the inelastic scattering as quasifree scattering from pointlike constituents within the proton, when viewed from a frame in which the proton has infinite momentum. The electron-proton center-of-mass frame is, at high energies, a good approximation of such a frame. In the infinite-momentum frame, the proton is Lorentz-contracted into a thin pancake, and the lepton scatters instantaneously. Furthermore, the proper motion of the constituents, of partons, within the proton is slowed down by time dilatation. We can estimate the interaction time and the lifetime of the virtual states within the proton. By using the notation of Fig. 1, we find the following.

Time of interaction:

$$\tau \approx 1/q^0 = 4P/(2M\nu - Q^2), \quad (2.1)$$

where q^0 was calculated in the lepton-proton center-of-mass frame.

Lifetime of virtual states:

$$T = \{[(xP)^2 + \mu_1^2]^{1/2} + [(1-x)^2P^2 + \mu_2^2]^{1/2} - [P^2 + M_p^2]^{1/2}\}^{-1} \\ = \frac{2P}{(\mu_1^2 + p_{1\perp}^2)/x + (\mu_2^2 + p_{2\perp}^2)/(1-x) - M_p^2}. \quad (2.2)$$

If we now require that

$$\tau \ll T, \quad (2.3)$$

then we can consider the partons, contained in the proton, as free during the interaction. Furthermore, if we consider large momentum transfers $-q^2 \gg M^2$, then we expect the scattering from the individual partons to be incoherent. The above conditions appear to be satisfied in the high-energy, large-momentum-transfer experiments at SLAC.

The kinematics for e - p inelastic scattering have been discussed in many places, in as many different nota-

* Work supported by the U. S. Atomic Energy Commission.

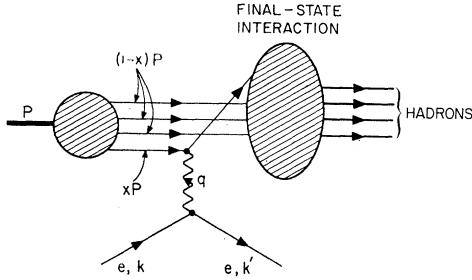


FIG. 1. Kinematics of lepton-nucleon scattering in the parton model.

tions.¹ We recall here that

$$\frac{EE'}{\pi} \frac{d\sigma}{dq^2 d\nu} = \frac{d\sigma}{d\Omega dE'} = \frac{\alpha^2}{4E^2 \sin^4(\frac{1}{2}\theta)} \times [W_2 \cos^2(\frac{1}{2}\theta) + 2W_1 \sin^2(\frac{1}{2}\theta)], \quad (2.4)$$

where W_1 and W_2 are functions of the two invariants

$$\begin{aligned} \nu &= (E - E') = q \cdot P / M, \\ Q^2 &= -q^2 = 4EE' \sin^2(\frac{1}{2}\theta), \end{aligned} \quad (2.5)$$

evaluated in the laboratory frame. The ratio W_1/W_2 is bounded. Using

$$\frac{W_1}{W_2} = \left(1 + \frac{\nu^2}{Q^2}\right) \frac{\sigma_t}{\sigma_t + \sigma_l}, \quad (2.6)$$

and the approximation $\frac{1}{2}\theta \ll 1$, we can write

$$\frac{d\sigma}{d\Omega dE'} \cong \frac{\alpha^2}{4E^2 \sin^4(\frac{1}{2}\theta)} W_2(q^2, \nu) \left[1 + \left(\frac{\sigma_t}{\sigma_t + \sigma_l}\right) \frac{\nu^2}{2EE'}\right], \quad (2.7)$$

where σ_t and σ_l (≥ 0) are the absorption cross sections for transverse and longitudinal photons.²

It remains to calculate the invariant functions W_1 and W_2 , especially W_2 . Within the model, the virtual photon interacts with one of the partons, while the rest remain undisturbed during the interaction. The interaction with the parton is as if the parton were a free, structureless particle. The cross section $d\sigma/d\Omega dE'$ is then a sum over individual electron-parton interactions appropriately weighted by the parton charge and momentum. For a free particle of any spin and unit charge, elementary calculation yields

$$W_2(\nu, q^2) = \delta(\nu - Q^2/2M) = M \delta(q \cdot P - \frac{1}{2}Q^2), \quad (2.8)$$

while for W_1 , we have

$$\begin{aligned} \sigma_t &= 0 \quad \text{for spin } 0, \\ \sigma_l &= 0 \quad \text{for spin } \frac{1}{2}, \end{aligned} \quad (2.9)$$

with an indeterminate result for higher spins.

¹ S. Drell and J. Walecka, *Ann. Phys. (N. Y.)* **28**, 18 (1964); J. D. Bjorken, *Phys. Rev.* **179**, 1547 (1969).

² L. Hand, in *Proceedings of the Third International Symposium on Electron and Photon Interaction at High Energies, Stanford Linear Accelerator Center, 1967* (Clearing House of Federal Scientific and Technical Information, Washington, D. C., 1968).

At infinite momentum, we visualize the intermediate state from which the electron scatters as follows:

(a) It consists of a certain number N of free partons (with probability P_N).

(b) The longitudinal momentum of the i th parton is a fraction x_i of the total momentum of the proton:

$$\mathbf{p}_i = x_i \mathbf{P}. \quad (2.10)$$

(c) The mass of the parton, before and after the collision, is small (or does not significantly change).

(d) The transverse momentum of the parton before the collision can be neglected, in comparison with $\sqrt{Q^2}$, the transverse momentum imparted as $p \rightarrow \infty$.

With these assumptions, it should be a good approximation to write, at infinite momentum,

$$\mathbf{p}_i^\mu \cong x_i \mathbf{P}^\mu. \quad (2.11)$$

The question of corrections to this approximation has been studied by Drell, Levy, and Yan.³ We shall not consider them further here.

The contribution to W_2 from a single parton of momentum $x\mathbf{P}^\mu$ and charge Q_i is then

$$\begin{aligned} W_2^{(i)} &= x_i Q_i^2 M \delta(q \cdot x_i P - \frac{1}{2}Q^2) \\ &= Q_i^2 M \delta\left(q \cdot P - \frac{Q^2}{2x_i}\right) = Q_i^2 \delta\left(\nu - \frac{Q^2}{2Mx_i}\right). \end{aligned} \quad (2.12)$$

The factor x_i in front is necessary to ensure that

$$\lim_{E \rightarrow \infty} \frac{d\sigma^{(i)}}{dq^2} = Q_i^2 \left(\frac{4\pi\alpha^2}{q^4}\right), \quad (2.13)$$

consistent with the Rutherford formula. For a general distribution of partons in the proton, we have

$$\begin{aligned} W_2(\nu, q^2) &= \sum_N P(N) \langle \sum_i Q_i^2 \rangle_N \\ &\times \int_0^1 dx f_N(x) \delta\left(\nu - \frac{Q^2}{2Mx}\right). \end{aligned} \quad (2.14)$$

Here $P(N)$ is the probability of finding a configuration of N partons in the proton, $\langle \sum_i Q_i^2 \rangle_N$ equals the average value of $\sum_i Q_i^2$ in such configurations, and $f_N(x)$ is the probability of finding in such configurations a parton with longitudinal fraction x of the proton's momentum, that is, with four-momentum $x\mathbf{P}^\mu$.

Upon integrating over x , we find

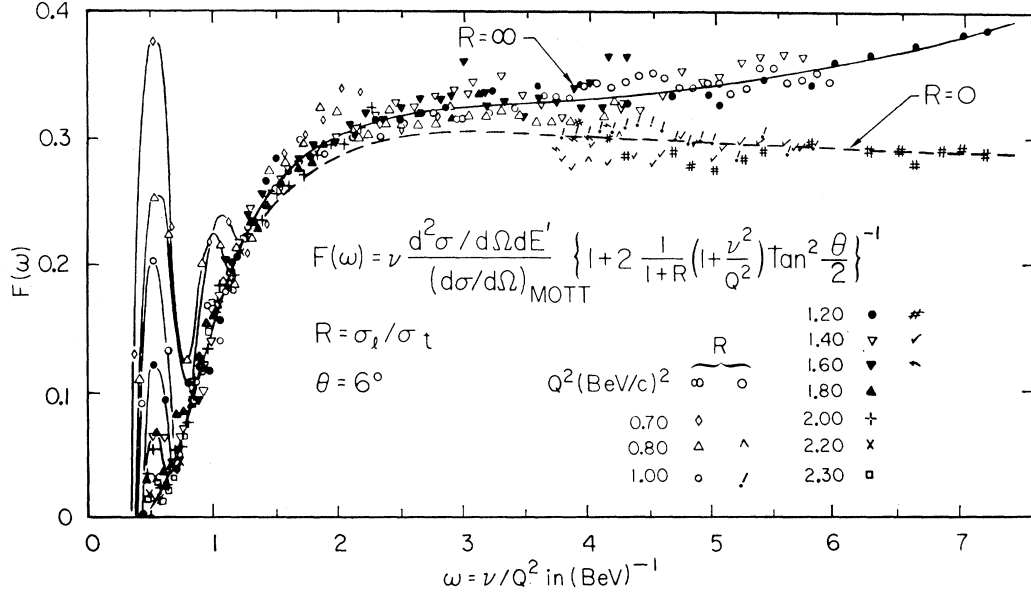
$$\nu W_2(\nu, q^2) = \sum_N P(N) \langle \sum_i Q_i^2 \rangle_N x f_N(x) \equiv F(x), \quad (2.15)$$

with

$$x = Q^2/2M\nu. \quad (2.16)$$

Therefore νW_2 is predicted to be a function of a *single*

³ S. D. Drell, D. J. Levy, and T.-M. Yan (private communication).


 FIG. 2. Plot of the data as a function of ν/Q^2 .

variable ν/Q^2 , a feature apparently satisfied by the data.⁴ Furthermore, the model provides an interpretation of the nature of the function $F(x)/x$: It is the mean square of the charge of partons with four-momentum xP^μ . The experimental⁴ determination of $F(x)$ is shown in Fig. 2.

Before going into detailed models for $f_N(x)$, we notice that

$$f_N(x_1) = \int dx_2 \cdots dx_N f_N(x_1, \cdots, x_N) \delta(1 - \sum_i x_i), \quad (2.17)$$

$$\int_0^1 dx_1 f_N(x_1) = 1,$$

where $f_N(x_1, \cdots, x_N)$ is the joint probability of finding partons (irrespective of charge) with longitudinal fractions x_1, \cdots, x_N . It follows that f_N is a symmetric function of its arguments. Therefore,

$$\begin{aligned} \int_0^1 x_1 dx_1 f_N(x_1) &= \frac{1}{N} \int dx_1 \cdots dx_N (\sum_i x_i) \\ &\quad \times f_N(x_1, \cdots, x_N) \delta(1 - \sum_i x_i) \\ &= 1/N. \end{aligned} \quad (2.18)$$

Putting together (2.18) and (2.15), we obtain a sum rule

$$\int dx F(x) = \sum_N P(N) \langle \sum_i Q_i^2 \rangle_N / N = \text{mean-square charge per parton}. \quad (2.19)$$

⁴ See the rapporteur talk of W. H. K. Panofsky, in *Proceedings of the Fourteenth International Conference on High-Energy Physics, Vienna, 1968* (CERN, Geneva, 1968), pp. 36-37, based on the work of E. Bloom, D. Coward, H. DeStaebler, J. Drees, J. Litt, G. Miller, L. Mo, R. Taylor, M. Breidenbach, J. Friedman, G. Hartmann, H. Kendall, and S. Loken.

Numerically,

$$\frac{Q^2}{2M} \int \frac{d\nu}{\nu} W_2 = \int dx F(x) \approx 0.16, \quad (2.20)$$

yielding a rather small mean-square charge per parton.

In the following models, out of ignorance, we shall choose one-dimensional phase space for the distribution function $f_N(x_1 \cdots x_N)$; that is,

$$f_N(x_1 \cdots x_N) = \text{const.} \quad (2.21)$$

An elementary calculation yields

$$f_N(x) = (N-1)(1-x)^{N-2}. \quad (2.22)$$

A. Three-Quark Model

Assuming that the proton is made up of three quarks with the usual charges,⁵ we obtain

$$\nu W_2 = f_3(x) = 2x(1-x), \quad x = Q^2/2M\nu. \quad (2.23)$$

While the data support $\nu W_2 \rightarrow \text{const}$ as $\nu \rightarrow \infty$ (or $x \rightarrow 0$), the model predicts that νW_2 should vanish, a result not dependent on the specific choice of $f_3(x)$, but only on the fact that f_3 is normalizable. In fact, within our one-dimensional model, if the number of partons is held finite, then the cross section vanishes as $x \rightarrow 0$. If, and only if,

$$\lim_{N^2 \rightarrow \infty} N^2 P(N) = \text{const} \neq 0 \quad (2.24)$$

will νW_2 approach a constant as $x \rightarrow 0$ ($\nu/Q^2 \rightarrow \infty$). This is shown in the Appendix.

⁵ M. Gell-Mann, *Phys. Letters* **8**, 214 (1964); C. Zweig, CERN Report Nos. TH 401, 402, 1964 (unpublished).

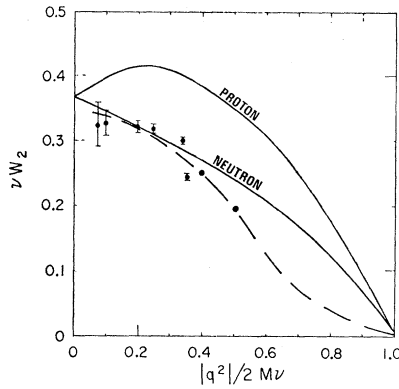


FIG. 3. Plot of the results for a model of three quarks in a sea of quark-antiquark pairs. The dashed line is visual fit through the experimental points of Ref. 4.

B. Three Quarks in a Background of Quark-Antiquark Pairs

In order to try to improve the model, we assume that in addition to the three quarks there is a distribution of quark-antiquark pairs (the "pion cloud"?). The mean-square charge of the cloud we take to be statistical

$$\langle \sum Q_i^2 \rangle_{\text{cloud}}/N = \frac{1}{3} \left[\left(\frac{2}{3}\right)^2 + \left(\frac{1}{3}\right)^2 + \left(\frac{1}{3}\right)^2 \right] = 2/9. \quad (2.25)$$

Therefore,

$$\begin{aligned} \langle \sum_i Q_i^2 \rangle_N &= 1 + 2/9(N-3) = 2/9N + \frac{1}{3} \quad \text{for the proton} \\ &= \frac{2}{9} + 2/9(N-3) = 2/9N \quad \text{for the neutron.} \end{aligned} \quad (2.26)$$

For $P(N)$, we choose

$$P(N) = C/N(N-1), \quad (2.27)$$

on the grounds that it is simple and has the asymptotic behavior which makes $\nu W_2 \rightarrow \text{const}$ as $x \rightarrow 0$. Before we begin, we note, from (2.26) and (2.19), that

$$\begin{aligned} \int_0^1 dx F(x) &= \int_0^1 dx \nu W_2 = 2/9 + \frac{1}{3} \langle 1/N \rangle > 0.22 \quad (\text{proton}) \\ &= 2/9 = 0.22 \quad (\text{neutron}) \\ &\approx 0.16 \quad (\text{expt.}). \end{aligned} \quad (2.28)$$

Thus we cannot expect a fit better than $\sim 50\%$ to the data. Inserting (2.27), (2.26), and (2.22) into the expression (2.15) for $F(x)$, we can perform the sum. For the proton,

$$\begin{aligned} F(x) &= x \sum_{N=3,5,\dots} P(N)(N-1)(1-x)^{N-2} (2/9N + \frac{1}{3}) \\ &= C \sum_{N=3,5,\dots} \left(\frac{2}{9} + \frac{1}{3N} \right) x (1-x)^{N-2} \\ &= C \left\{ \frac{2(1-x)}{9(2-x)} + \frac{1}{6} \frac{x}{(1-x)^2} \left[\ln \left(\frac{2-x}{x} \right) - 2(1-x) \right] \right\}. \end{aligned} \quad (2.29)$$

The normalization constant C is determined from the condition

$$1 = \sum_{N=3,5,\dots} P_N(x) = C \sum_{N=3,5,\dots} \frac{1}{N(N-1)} = C(1-\ln 2). \quad (2.30)$$

For the neutron, the term in square brackets is omitted; thus the final expressions are

$$\begin{aligned} F_p(x) &= \frac{1}{1-\ln 2} \left\{ \frac{2(1-x)}{9(2-x)} + \frac{1}{6} \frac{x}{(1-x)^2} \right. \\ &\quad \left. \times \left[\ln \left(\frac{2-x}{x} \right) - 2(1-x) \right] \right\}, \end{aligned} \quad (2.31)$$

$$F_n(x) = \frac{2}{9(1-\ln 2)} \left(\frac{1-x}{2-x} \right).$$

It is clear that the results are model-dependent and not to be taken too seriously. There is a need for a model-independent check of the basic assumptions. In Sec. III we discuss the corresponding process with electrons replaced by γ rays as a test of the basic idea of the calculation.

In Fig. 3, we compare Eqs. (2.31) with the experiment. The shape of the curve is in fair agreement, and could be improved by suppressing the contribution of three-parton configurations. On the other hand, the over-all normalization is off, as discussed below [(2.28)]. Readjustment of the coefficients P_N or the distributions $f_N(x)$ of longitudinal fraction cannot improve this feature. The ratio of neutron cross section to proton remains nearly constant and about 0.8 over a large range of x , although the ratio approaches 1 as $x \rightarrow 0$.

According to (2.9), if the partons all have spin $\frac{1}{2}$, we expect $\sigma_l/\sigma_t \rightarrow 0$; if they are spinless, we find instead $\sigma_l/\sigma_t \rightarrow 0$. A finite ratio would indicate that both kinds are present.

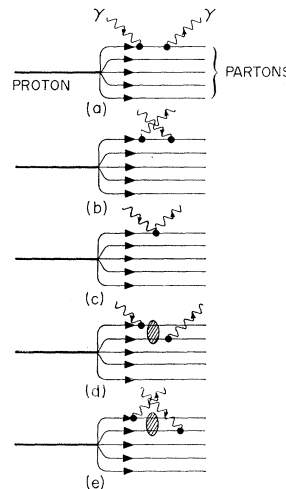


FIG. 4. Diagrams contributing to inelastic Compton scattering.

III. INELASTIC COMPTON SCATTERING

In this section, we suggest that a good way to find out about the internal structure of the proton is to look at it. That is, one should measure the inelastic scattering of photons from protons, yielding a photon plus anything else. The yield can be predicted in terms of this model. We visualize the inelastic scattering again as incoherent scattering from the partons in the proton according to the point cross section. The elementary photon-parton scattering goes by the diagrams shown in Fig. 4. Diagram (c) in Fig. 4, does not occur for spin- $\frac{1}{2}$ partons. Its contribution is evidently very similar to the case of electron scattering. We argue that exchange-terms such as in diagrams (d) and (e) can be ignored on the basis that the lifetime of the intermediate states, between absorption and emission of the photon, is of order $E_{e.m.}^{-1}$ in the γ -proton center-of-mass system and much less than the lifetime of the virtual-parton states of the proton estimated in (2.2). Furthermore, because we require the momentum transfer between the photons to be large (> 1 BeV/c), the parton will necessarily have transverse momentum much larger than the average momentum within the proton and the probability that it interacts with another parton within the proton at such high P_1 is very small.

The kinematics for the process is illustrated in Fig. 5, with the value

$$\begin{aligned} s &= (k+p)^2 \approx 2k \cdot p = (2Mk)_{lab} \gg M^2, \\ t &= (k-k')^2 = -2k \cdot k' = -[4kk' \sin^2(\frac{1}{2}\theta)]_{lab}, \quad (3.1) \\ M\nu &= (k-k') \cdot p = M(k-k')_{lab}, \\ u &\approx -s-t. \end{aligned}$$

We require $-t$ to be large, as we already mentioned, so that the process is incoherent, and only Figs. 4(a)-4(c) (for integer spin) need be taken into account. The method for calculation is the same as in Sec. II: We take the Compton cross section from point partons and average over the parton momentum distributions and proton configurations. This elementary photon-parton interaction is given (for spin- $\frac{1}{2}$ partons) by the Klein-Nishina formula written in terms of the Mandelstam variables s, t, u . If the parton carries the full momentum $P(x=1)$, we have

$$\begin{aligned} \frac{d\sigma}{dt d\nu} &= \frac{4\pi\alpha^2}{s^2} \delta\left(\nu + \frac{t}{2M}\right) Q_i^4 \quad \text{for spin } 0 \\ &= \frac{-2\pi\alpha^2}{s^2} \left(\frac{s}{u} + \frac{u}{s}\right) \delta\left(\nu + \frac{t}{2M}\right) Q_i^4 \quad \text{for spin } \frac{1}{2}, \quad (3.2) \end{aligned}$$

which can be combined into the form

$$\frac{d\sigma}{dt d\nu} = \frac{4\pi\alpha^2}{s^2} \left(1 - R \frac{(s+u)^2}{2su}\right) \delta\left(\nu + \frac{t}{2M}\right) Q_i^4, \quad (3.3)$$

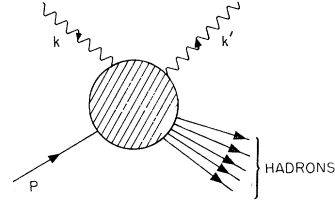


FIG. 5. Kinematics of Compton scattering.

with

$$\begin{aligned} R &= 1 \quad \text{for spin } \frac{1}{2} \\ &= 0 \quad \text{for spin } 0. \end{aligned} \quad (3.4)$$

If the parton has longitudinal fraction x , we make the replacements (we are here in the infinite-momentum frame)

$$\begin{aligned} s &\rightarrow xs, \quad u \rightarrow xu, \quad t \rightarrow t, \\ \delta(\nu + t/2M) &\rightarrow \delta(\nu + t/2Mx). \end{aligned} \quad (3.5)$$

We then multiply by the distribution function $f_N(x)$ and by $P(N)$, integrate over x , and sum over N [cf. Eqs. (2.12)-(2.15)] to obtain

$$\begin{aligned} \frac{d\sigma}{dt d\nu} &= \sum_N \int_0^1 dx P(N) f_N(x) \frac{4\pi\alpha^2}{x^2 s^2} \\ &\times \left[1 - R \frac{(s+u)^2}{2su}\right] \delta\left(\nu + \frac{t}{2Mx}\right) \langle \sum_i Q_i^4 \rangle_N. \end{aligned} \quad (3.6)$$

Integrating over x and expressing the result in laboratory variables, Eq. (3.1) gives the final result:

$$\begin{aligned} \frac{d\sigma}{d\Omega dk' k'} &= \frac{\alpha^2}{4k' \sin^4(\frac{1}{2}\theta)} \frac{\nu}{kk'} \left[1 + R \frac{\nu^2}{2kk'}\right] \\ &\times \sum_N P(N) x f_N(x) \langle \sum_i Q_i^4 \rangle_N, \end{aligned} \quad (3.7)$$

with

$$x = -t/2M\nu. \quad (3.8)$$

Making the identification

$$k \leftrightarrow E, \quad k' \leftrightarrow E', \quad -t \leftrightarrow Q^2, \quad R \leftrightarrow \sigma_t/(\sigma_t + \sigma_l), \quad (3.9)$$

we find a remarkable correspondence between (3.7) and (2.14), (2.9), and (2.7), the corresponding cross section for electrons. The only changes are the additional factor ν^2/kk' and the replacement $Q_i^2 \rightarrow Q_i^4$. Even the factor in square brackets dependent on parton spin is the same. We conclude that within the validity of this parton model, for partons of unit charge ($Q^2 = Q^4$) and spin 0 or $\frac{1}{2}$, the ratio of electron scattering to γ scattering is a model-independent number of order

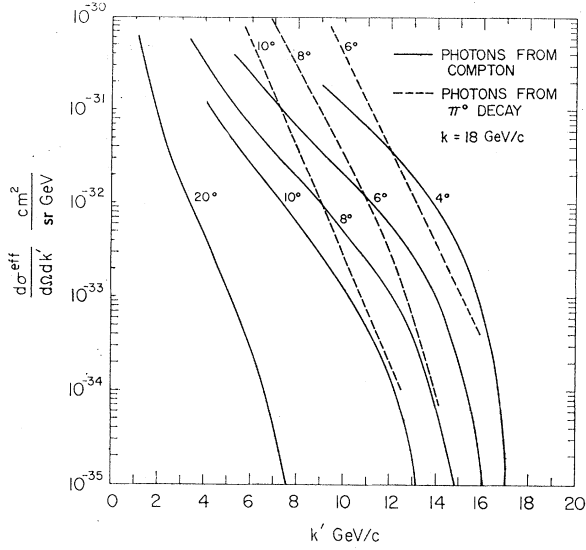


FIG. 6. Double-differential laboratory cross section for inelastic Compton scattering for an 18-GeV incident bremsstrahlung spectrum. The solid curve corresponds to the signal. The dotted curve is the background of γ 's from π^0 's using the data of Ref. 8 as discussed in the text.

unity. In general,⁶

$$\left(\frac{d\sigma}{d\Omega dE'}\right)_{\gamma p} = \frac{\nu^2}{kk'} \left(\frac{d\sigma}{d\Omega dE'}\right)_{ep} \frac{\langle \sum_i Q_i^4 \rangle}{\langle \sum_i Q_i^2 \rangle}, \quad (3.10)$$

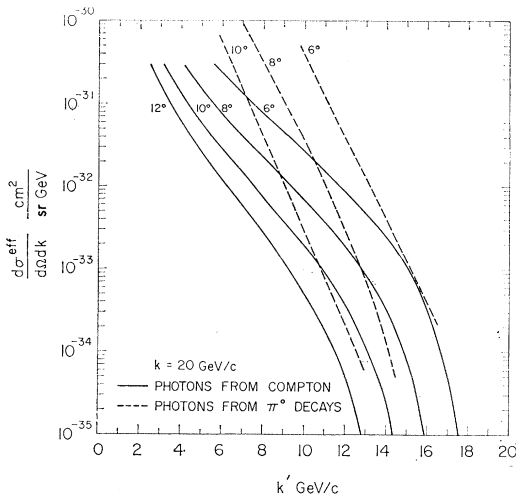


FIG. 7. Inelastic Compton scattering for a 20-GeV incident bremsstrahlung spectrum. The background curves are the same as in Fig. 6.

⁶ We point out that the argument used in Sec. II in deriving the sum rule can be repeated here, giving

$$Q^2 \int \left(\frac{d\sigma}{d\Omega dE'}\right)_{\gamma p} \frac{kk'}{\nu^2 \sigma_R} d\nu = \sum_N P(N) \langle \sum_i Q_i^4 \rangle_N / N,$$

where $\sigma_R = [\alpha^2/4k^2 \sin^4(\frac{1}{2}\theta)](1 + R\nu^2/2kk')$. We have also assumed the same momentum distribution $f_N(x)$ for the spin-0 and spin- $\frac{1}{2}$ partons.

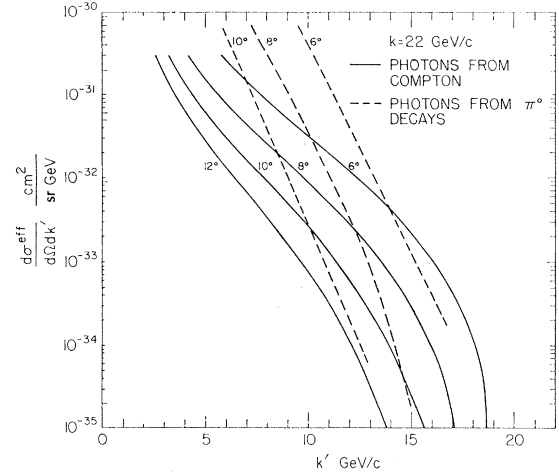


FIG. 8. Inelastic Compton scattering for a 22-GeV incident bremsstrahlung spectrum. The background curves are the same as in Fig. 6.

where for any operator $O(N)$ we have

$$\langle O \rangle = \sum_N P(N) O(N) f_N(x). \quad (3.11)$$

For our model of three quarks in a cloud of quark-antiquark pairs, there exist upper and lower limits for $\langle \sum Q_i^4 \rangle / \langle \sum Q_i^2 \rangle$. We note from (2.25) and (2.26), for the proton, that

$$\begin{aligned} \langle \sum_i Q_i^4 \rangle_N &= \frac{11}{27} + \frac{2}{27}(N-3) = \frac{1}{3} \langle \sum_i Q_i^2 \rangle_N + \frac{2}{27} \\ &= \frac{5}{9} \langle \sum_i Q_i^2 \rangle_N - \frac{4}{81} N. \end{aligned} \quad (3.12)$$

Therefore, for identical kinematical regions⁷ we have

$$\frac{1}{3} \frac{\nu^2}{EE'} \left(\frac{d\sigma}{d\Omega dE'}\right)_{ep} < \left(\frac{d\sigma}{d\Omega dE'}\right)_{\gamma p} < \frac{5}{9} \frac{\nu^2}{EE'} \left(\frac{d\sigma}{d\Omega dE'}\right)_{ep}. \quad (3.13)$$

In principle it should be possible, if the model is correct, to distinguish between fractional and integer-charged partons.

IV. BACKGROUND AND RATE ESTIMATES FOR INELASTIC γ -RAY EXPERIMENT

We consider an experiment in which a bremsstrahlung beam is sent through hydrogen and the inelastically scattered γ ray is detected with momentum k' at angle θ . The main problem, in principle, is to differentiate the Compton γ rays from the γ rays coming from the decays of photoproduced π^0 's. Here, we calculate the effective

⁷ These bounds depend on the implicit assumptions of Eq. (2.25). A smaller lower bound of $\frac{1}{3}$ is obtained if we assume that all the pairs are made up of charges $\frac{1}{3}$ and $-\frac{1}{3}$.

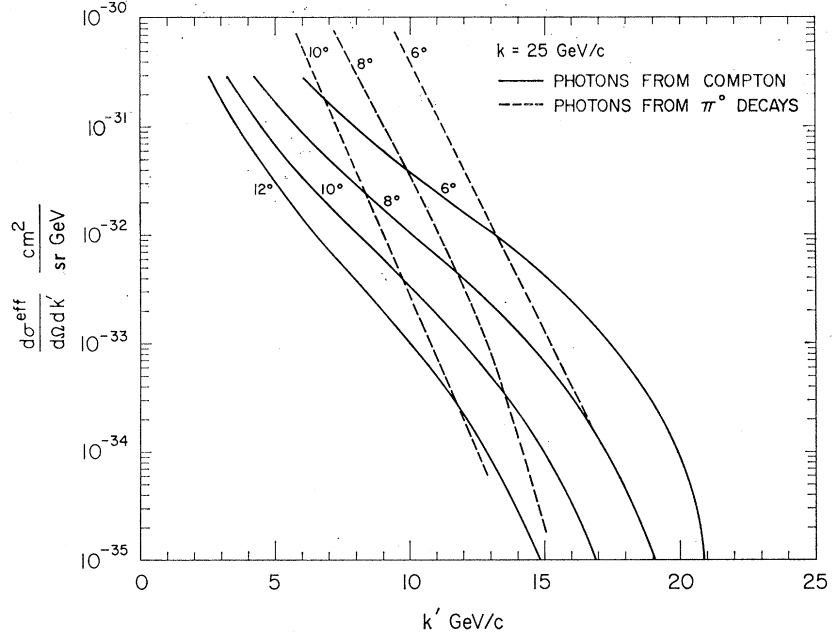


FIG. 9. Inelastic Compton scattering for a 25-GeV incident bremsstrahlung spectrum. The background curves are the same as in Fig. 6.

cross section for the production of Compton-scattered γ rays by folding the Compton cross section over the bremsstrahlung spectrum. We then calculate for comparison the corresponding background γ rays, estimated at SLAC from the beam survey experiments⁸ for charged π 's. We define

$$\frac{d\sigma^{\text{eff}}}{d\Omega dk'} = \int_{k'+|t|/2M}^E \frac{\text{electron } dk}{k} \frac{d\sigma_{\gamma p}}{d\Omega dk'} \quad (4.1)$$

We assume, optimistically, that the partons have unit charge and spin $\frac{1}{2}$; from (3.3) and (4.1) we obtain

$$\frac{d\sigma^{\text{eff}}}{d\Omega dk'} = \frac{4\alpha^2}{M^2 k'} \int_{1/2}^{M(E-k')/4Ek' \sin^2(\frac{1}{2}\theta)} \lambda d\lambda F(\lambda) \times \left[1 - \frac{4k'\lambda \sin^2(\frac{1}{2}\theta)}{M} + \frac{8k'^2 \lambda^2 \sin^4(\frac{1}{2}\theta)}{M^2} \right], \quad (4.2)$$

with

$$\lambda = M\nu/Q^2. \quad (4.3)$$

We have calculated this expression for several incident electron energies as a function of k' and θ , using for $F(\lambda)$ the values given in Ref. 2. The results are shown as Figs. 6–9. In the same figures are shown our estimates of the corresponding background from the decay of photoproduced π^0 's into γ rays. The estimate was made by assuming that the yield of π^+ measured in the SLAC beam survey experiment⁸ equals the π^0 yield. We thereby obtain, for the effective cross section

per nucleon,

$$\begin{aligned} \left(\frac{d\sigma_{\pi}}{d\Omega dk'} \right)_{\text{eff}} &= (\text{yield})_{\pi^+} / 0.7 \int_{t=0}^{0.3} t dt \text{ (g/rad length of Be)} \\ &\quad \times (\text{Avogadro No.}) \\ &= 8.2 \times 10^{-25} (\text{yield})_{\pi^+} \text{ cm}^2/\text{sr BeV}. \end{aligned} \quad (4.4)$$

The terms in the denominator have the following origin: The thin-target bremsstrahlung spectrum is tdk/k , where t is the thickness in radiation lengths (r.l.) (the target was 0.3 r.l. Be). The factor 0.7 is a thick-target correction calculated by Tsai and Van Whitis.⁹ $(\text{Yield})_{\pi^+}$ is taken from the SLAC User's Handbook⁸ and the γ -ray flux is obtained by folding the π^0 -decay spectrum into (4.4):

$$\begin{aligned} \left(\frac{d\sigma}{d\Omega dk'} \right)_{\gamma} &= 2 \int_{k_{\gamma}}^E \left(\frac{d\sigma_{\pi}}{d\Omega dk'} \right)_{\text{eff}} \frac{dk'}{k'} \approx \frac{2}{k_{\gamma}} \int_{k_{\gamma}}^{\infty} \left(\frac{d\sigma_{\pi}}{d\Omega dk'} \right)_{\text{eff}} dk' \\ &\approx (2E_0/k_{\gamma}\theta) (8.2 \times 10^{-25}) (\text{yield})_{\pi^+} \\ &\quad \text{(as function of } k_{\gamma}), \end{aligned} \quad (4.5)$$

where in the last step we have used the empirical observation that

$$d\sigma_{\pi}/d\Omega dk' \sim e^{-k'\theta/E_0}, \quad (4.6)$$

with

$$E_0 \approx 0.154 \text{ BeV.}$$

In Figs. 6–9, the background is that from an 18-BeV bremsstrahlung beam. It is expected that this background increases slowly with beam energy, and keeps

⁸ SLAC User's Handbook, Sec. D.1, Figs. 1 and 2 (unpublished).

⁹ Y. S. Tsai and Van Whitis, Phys. Rev. **149**, 1948 (1966).

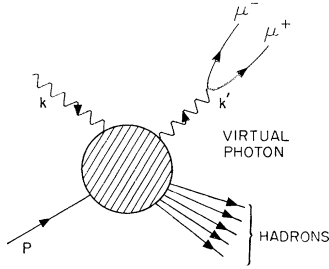


FIG. 10. Muon-pair production by inelastic Compton scattering.

the same shape, in particular, the exponential dependence on transverse momentum. However, as the primary electron energy increases, the γ -ray spectrum from the inelastic Compton process, if it exists, is displaced upward in energy, so that for 20-BeV electrons and above, there is a region where the Compton signal dominates the π^0 noise. In any case, it will certainly be necessary to compare the γ -ray spectrum with that of the π^+ under the same conditions as reassurance that Compton γ rays are indeed being seen.

A variation of this experiment is to consider the inelastic Compton terms in μ -pair photoproduction (see Fig. 10). We have not analyzed this process in detail. The rate is diminished by a factor roughly¹⁰ $\sim (2\alpha/3\pi)[\ln(E_{\max}/m_\mu) - 3.5] \sim 1/350$ but if the charged pions are absorbed immediately downstream from the target, the background muon flux from π^\pm decay can be reduced by a factor $\sim 1/700$ as well. Furthermore, the two muons are strongly correlated in angle, providing a quite unique signature. All this is encouragement that perhaps the background is manageable. The "singles" background from the Bethe-Heitler diagrams, for which the undetected muon predominantly goes in the forward direction, is interesting, as well, and very likely exceeds the singles rate from Compton μ pairs. But this is also of interest in testing μ - e universality at very high q^2 . The "Bethe-Heitler" muons probably dominate the background muons from π^+ decay, but the necessary estimates have not yet been made.

APPENDIX

We attain a condition between $P(N)$ and $\langle \sum_i Q_i^2 \rangle_N$ which guarantees that $F(x)$ is analytic at $x=0$ and equal to a nonzero constant. Using the Sommerfeld-Watson transformation, we rewrite (2.15) as an integral

¹⁰ R. H. Dalitz, Proc. Phys. Soc. (London) A64, 667 (1951).

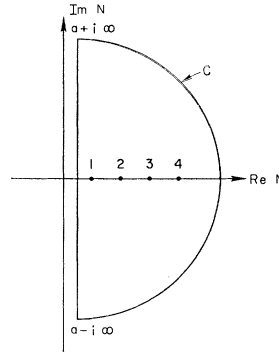


FIG. 11. Contour of integration for the Sommerfeld-Watson transform.

over the contour shown in Fig. 11:

$$F(x) = 2x \int_c NP(2N+1) \langle \sum_i Q_i^2 \rangle_{(2N+1)} \frac{(1-x)^{2N-1} e^{i\pi N}}{\sin \pi N} dN. \quad (\text{A1})$$

The contribution of the semicircle at infinity is negligible. For what remains in the integral, we can use (for $x \rightarrow 0$)

$$x(1-x)^{2N-1} \approx x e^{-(2N-1)x} = -\frac{1}{2} \partial e^{-(2N-1)x} / \partial N, \quad (\text{A2})$$

and integrate by parts:

$$F(x) = \int_{a-i\infty}^{a+i\infty} e^{-(2N-1)x} \frac{\partial}{\partial N} \left[\frac{NP(2N+1) \langle \sum_i Q_i^2 \rangle_{(2N+1)} e^{i\pi N}}{\sin \pi N} \right] dN. \quad (\text{A3})$$

In the limit of $x \rightarrow 0$, we have

$$F(x) \longrightarrow \frac{NP(2N+1) \langle \sum_i Q_i^2 \rangle_{(2N+1)} e^{i\pi N}}{\sin \pi N} \Big|_{a-i\infty}^{a+i\infty} \longrightarrow_{N \rightarrow a-i\infty} NP(2N+1) \langle \sum_i Q_i^2 \rangle_{(2N+1)}. \quad (\text{A4})$$

Therefore $F(x)$ approaches a constant if and only if $P(N) \rightarrow c/N \langle \sum_i Q_i^2 \rangle_N$. For $\langle \sum_i Q_i^2 \rangle_N$ linear in N , this reduces to the condition mentioned in the text.

ACKNOWLEDGMENTS

We thank R. P. Feynman, J. Weyers, and our colleagues at SLAC for many helpful conversations.